

# Characterization of Commercial Linear Low-Density Polyethylene by TREF-DSC and TREF-SEC Cross-Fractionation

MINGQIAN ZHANG, DAVID T. LYNCH, SIEGHARD E. WANKE

Department of Chemical and Materials Engineering, University of Alberta, Edmonton, Alberta, Canada T6G 2G6

Received 4 June 1999; accepted 11 August 1999

**ABSTRACT:** A new technique for characterization of linear low-density polyethylene (LLDPE) is presented in this report. The molecular structure of two commercial LLDPEs, produced by copolymerization of ethylene with 1-butene over a Ziegler-Natta and a metallocene catalyst, was investigated. The LLDPE resins were fractionated by temperature rising elution fractionation (TREF), and the TREF fractions were further analyzed by size exclusion chromatography and differential scanning calorimetry (DSC) coupled with successive nucleation/annealing (SNA). The cross-fractionation techniques provided detailed information about the molecular structure of different types of LLDPEs; of particular interest is the TREF-SNA-DSC cross-fractionation which allowed a direct observation of methylene sequence distribution and thus short chain branch (SCB) distribution. TREF-size exclusion chromatography cross-fractionation showed that the molar mass of the Ziegler-Natta LLDPE increased monotonically with decreasing SCB, whereas the plot of  $M_w$  vs SCB for the metallocene LLDPE showed a maximum. TREF-SNA-DSC cross-fractionation clearly showed that the metallocene LLDPE only had intramolecular heterogeneity in SCB distribution, whereas the Ziegler-Natta LLDPEs exhibited both intermolecular and intramolecular heterogeneity. © 2000 John Wiley & Sons, Inc. *J Appl Polym Sci* 75: 960–967, 2000

**Key words:** Ziegler-Natta and metallocene LLDPE; cross-fractionation; molecular microstructure; TREF; SEC; DSC

## INTRODUCTION

Linear low-density polyethylene (LLDPE), produced by the copolymerization of ethylene with  $\alpha$ -olefins over either Ziegler-Natta or metallocene catalysts, is a copolymer which possesses short chain branches (SCB) due to the incorporation of  $\alpha$ -olefins into the polymer backbone. It has been shown that such LLDPEs exhibit high heterogeneity in both molar mass and SCB distribution.<sup>1–3</sup>

The final thermal and mechanical properties are closely related to these heterogeneities.<sup>3,4</sup> Hence, the characterization of LLDPE with respect to molar mass and SCB by new and improved analytical techniques is of great interest.

Fractionation of LLDPE in terms of molar mass and SCB seems to be the best way to characterize the molecular structure of LLDPE. Size exclusion chromatography (SEC) has long been used to measure molar masses and molar mass distributions of polymer. Temperature rising elution fractionation (TREF), a technique that fractionates semicrystalline polymer according to crystallizability, has been widely used for the characterization of LLDPE with respect to SCB.<sup>1,2</sup> The extended use of TREF is the combi-

Correspondence to: S. E. Wanke.

Contract grant sponsors: Natural Sciences and Engineering Research Council of Canada and NOVA Chemicals Corporation.

*Journal of Applied Polymer Science*, Vol. 75, 960–967 (2000)

© 2000 John Wiley & Sons, Inc.

CCC 0021-8995/00/070960-08

**Table I Commercial LLDPEs Studied**

LLDPE	Manufacturer	Comonomer Type	Density	$M_w \cdot 10^{-4}$	$P_d$
Exact4033	Exxon	1-butene	0.880	11.0	2.14
PF0118F	NOVA	1-butene	0.918	10.6	3.28

$M_w$ , weight average molar mass;  $P_d$ , polydispersity ( $M_w/M_n$ ).

nation of TREF with another fractionation technique to further separate the molecular species according to their different structures. The cross-fractionation can, in essence, provide more detailed information about the molecular structure of LLDPE. TREF combined with SEC, or TREF-SEC cross-fractionation, has been used extensively to correlate SCB and molar mass of different LLDPEs.<sup>3,5-9</sup> The method has also become useful recently for obtaining kinetic characteristics of polymerization of ethylene on the heterogeneous catalyst system.<sup>10,11</sup>

Detailed information about SCB distribution, in particular, the intermolecular and intramolecular distribution of SCB, is of paramount importance in determining thermodynamic and crystallization behaviors of LLDPEs.<sup>12,13</sup> Such information can be obtained by compositional cross-fractionation. However, because of the lack of another compositional fractionation technique, relatively little has been reported on the intra- and intermolecular SCB distribution of TREF fractions and their generation mechanism. In recent years, thermally fractionated DSC has been developed into a compositional fractionation technique for LLDPE.<sup>14-19</sup> It should therefore be possible to combine TREF with DSC to obtain additional information on the molecular structure of different types of LLDPEs.

The objective of this report is to present results of the molecular structure of commercial LLDPEs produced by the Ziegler-Natta and metallocene catalysts. TREF-SEC cross-fractionation is used to characterize the relationship between SCB and molar mass. The TREF fractions are also segregated based on methylene sequence length by using DSC coupled with the successive nucleation/annealing (SNA) to reveal the heterogeneity of SCB distribution.

## EXPERIMENTAL

### Materials

The two commercial linear low-density polyethylenes used in this study are described in Table I.

Both LLDPEs were ethylene-butene copolymers having approximately the same weight-average molar masses but different polydispersities. PF0118F, from NOVA Chemicals Corp., Calgary, Canada, was produced on a Ziegler-Natta catalyst with the density of 0.918, whereas Exact4033, from Exxon Chemical Company, Houston, TX (density 0.880) was produced with a metallocene catalyst.

### TREF

The fractionation of LLDPE resins by TREF consists of crystallization and elution steps. The crystallization step involved dissolving the sample at 125°C in *o*-xylene at a concentration of 0.005–0.04 g PE/mL, followed by slowly cooling the polymer solution to approximately –8°C at a cooling rate of 1.5°C/h to allow the polymer to crystallize out of solution onto glass beads (80–100 mesh). The crystallized sample was filtered into a TREF column which was then connected to the TREF system. The elution step was operated in two different modes—analytical TREF (ATREF) and preparative TREF (PTREF). In ATREF, the column (9.5 mm in diameter and 63.5 mm in length) temperature was increased at a rate of 1°C/min while the solvent (*o*-dichlorobenzene) was pumped through the column continuously at a rate of 1.0 mL/min. The species eluting from the column were detected with an on-line infrared detector tuned at 2860 cm<sup>-1</sup>. In the case of PTREF, a bigger column with a diameter of 11.5 mm and length of 63.5 mm was used. The elution temperature range was divided into several temperature intervals based on the ATREF profile. The temperature of the column was raised in 10 min from lower to higher temperature of each interval and soaked at the high temperature for 10 min without solvent flowing; then the solvent was started to allow the dissolved polymer to elute from the column. The eluted polymer was monitored by the on-line infrared detector and was collected for SEC and DSC analysis.

### SNA and DSC

The LLDPE in the fractions collected from PTREF mentioned above was precipitated by adding 15 mL of acetone to the PTREF solution. The slurry was then filtered using 0.5- $\mu$ m Teflon film. The obtained polymer was washed thoroughly with acetone and dried at ambient temperature. The resulting sample was encapsulated in two aluminum DSC pans and was subjected to SNA treatment. To erase the previous thermal history, the sample was heated at a rate of 5°C/min up to 155°C for the Ziegler-Natta sample and 135°C for the metallocene sample and was maintained at that temperature for 10 min. The sample was subsequently cooled to 25°C at a cooling rate of 5°C/min to create the initial "standard" state.

The SNA procedure, which was similar to the so-called self-nucleation procedure,<sup>18,20</sup> included a series of heating-annealing-cooling cycles. The polymer samples or TREF fractions were heated at 5°C/min to a selected temperature and were maintained at that temperature for 10 min. This step results in the formation of partial melting and annealed crystal fragment. The crystallization was achieved by subsequently cooling the sample to 25°C at a cooling rate of 5°C/min. The heating-annealing-cooling cycle was repeated at a temperature interval of 5°C from 135 to 25°C for the Ziegler-Natta sample and 105 to 25°C for the metallocene sample. Detailed temperature history of the SNA for the Ziegler-Natta LLDPE is shown in Figure 1.

The DSC endotherms of the samples were measured using a TA Instrument Model DSC2910. The instrument was calibrated with an indium

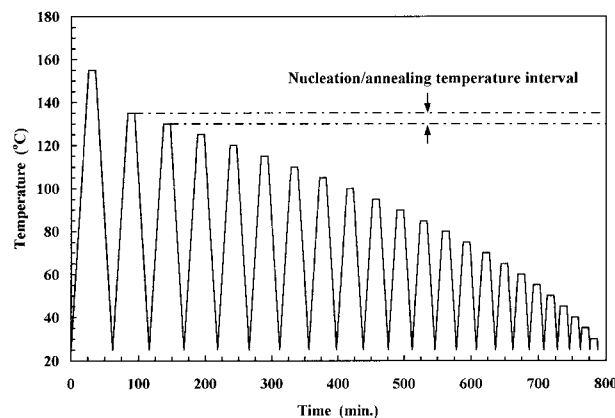


**Figure 1** Schematic representation of successive nucleation/annealing (SNA) for thermal fractionation of Ziegler-Natta LLDPE.

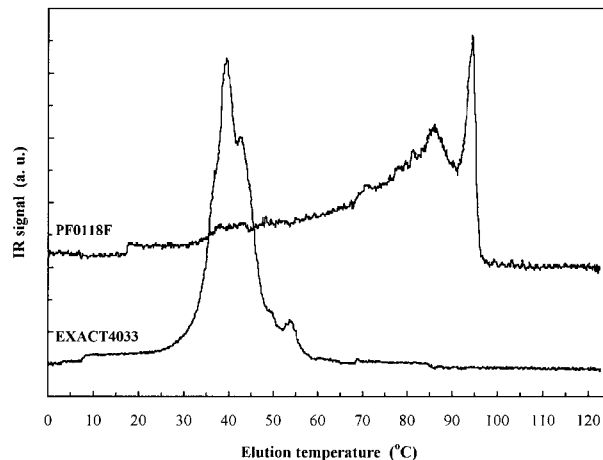


**Figure 2** ATREF profiles of Ziegler-Natta and metallocene LLDPEs.

standard. The LLDPE samples or PTREF fractions treated by SNA were heated from 0°C at a heating rate of 10°C/min to 160°C and subsequently cooled to 0°C at the same rate. The transition temperature and the degree of crystallinity were analyzed by the TA2200 software package.

### SEC

The molar mass distribution of the whole LLDPEs and TREF fractions was determined on a Waters 150C GPC equipped with a differential refractometer. The columns used for the separation were four Shodex columns UT 806M maintained at 140°C, and the solvent was 1,2,4-trichlorobenzene at a flow rate of 1.0 mL/min. Data were treated according to a universal calibration generated with narrow polystyrene and polyethylene standards.

## RESULTS

### TREF and SNA-DSC

Figure 2 shows ATREF profiles of the two LLDPEs. The metallocene LLDPE showed a narrow peak at elution temperatures ranging from 28 to 58°C, indicating a narrow SCB distribution. In comparison, the Ziegler-Natta ethylene-butene copolymer demonstrated a rather broad bimodal distribution, which is normally attributed to multiple active sites present on the Ziegler-Natta catalyst.<sup>2,3,7</sup>

A calibration curve relating TREF elution temperature to SCB content was established based on

**Table II Average Short Chain Branch Content Calculated from TREF Profiles**

LLDPE	$C_n$ (CH <sub>3</sub> /1000C)	$C_w$ (CH <sub>3</sub> /1000C)	$C_w/C_n$
PF0118F	17.7	26.5	1.50
Exact4033	32.4	33.3	1.02

the TREF-SEC cross-fractionation of a highly dispersed homopolyethylene.<sup>10</sup> Similar expressions to molar mass distribution based on moments were used to calculate number-average and weight-average SCB contents,  $C_n$  and  $C_w$ :

$$C_n = \frac{\sum A_i C_i}{\sum A_i}; \quad C_w = \frac{\sum A_i C_i^2}{\sum A_i C_i}$$

where  $A_i$  is the slice area of the TREF profile and  $C_i$  is the corresponding SCB evaluated from the calibration curve. The value of  $C_w/C_n$  can serve as an indicator of the broadness of SCB distribution. Table II gives the results of the Ziegler-Natta and metallocene LLDPEs. Note that the metallocene sample had higher SCB content, whereas the Ziegler-Natta sample showed a broader distribution, as evidenced by the ratio of  $C_w$  to  $C_n$ .

Figure 3 shows DSC endotherms of the two LLDPEs treated by SNA. The SNA-DSC is a temperature-dependent process that segregates macromolecules based on recrystallization and reorganization of methylene sequences from the melt. It is, in principle, similar to other thermally-fractionated DSC,<sup>14–19</sup> but is much more efficient and offers higher resolution.<sup>18</sup> The neighboring sequence on the polymer chain can crystallize independently and subsequently melt at a temperature corresponding to its crystallite size. As a result, each peak of SNA-DSC endotherms represents a group of methylene sequences of equal or similar length. It can be seen from Figure 3 that the SNA-DSC is capable of differentiating between methylene sequence distribution in the two samples. The Ziegler-Natta LLDPE showed a broader methylene sequence distribution than the metallocene LLDPE, and the methylene sequence distribution resembled the TREF profiles.

### TREF-SEC Cross-Fractionation

The ATREF data in Figure 2 shows that for the Ziegler-Natta sample, the polymer concentration eluted is very low at low elution temperatures and very high at high elution temperatures. This

posed a problem for collecting representative TREF fractions in a single PTREF run which can be used subsequently for SEC and DSC analysis. A large sample size is necessary to collect an adequate amount of sample at low temperatures for subsequent DSC analysis, but it causes problems such as solvent flow blockage and incomplete dissolving of polymer because of the limited volume of the column. To overcome these problems, two PTREF runs with varied sample sizes were performed to ensure that the PTREF fractions collected were representative. At first, a sample size of 300 mg was used which allowed TREF fractions to be collected in a temperature range typical of the branched polymer (0–85°C) as indicated in Figure 2. On the second PTREF run, a smaller sample size (60 mg) was used to collect fractions at high temperatures (85–100°C). Figure 4 shows the molar mass distribution of the collected PTREF fractions. The number and weight average molar mass as well as polydispersity index are given in Table III. It is evident in Figure 4 that all eight fractions showed similar shape of molar mass distribution. The distribution curve shifted toward higher molar masses with increasing TREF elution temperatures, as shown in Table III. The polydispersity index  $M_w/M_n$  seemed to slightly decrease as the elution temperature increased.

Unlike the Ziegler-Natta sample, the whole metallocene sample can be separated easily into six fractions by PTREF. Figure 5 shows the molar mass distribution of the PTREF fractions and Table IV gives the molar masses and polydispersity of each fraction. The molar mass distribution curves for the fractions eluted at temperatures

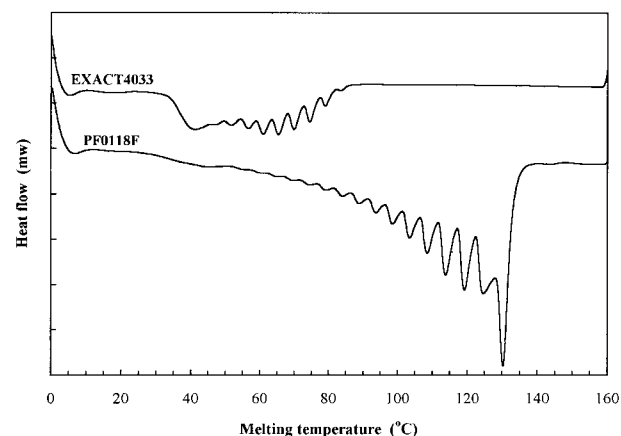


**Figure 3** DSC endotherms of Ziegler-Natta and metallocene LLDPEs treated by SNA.

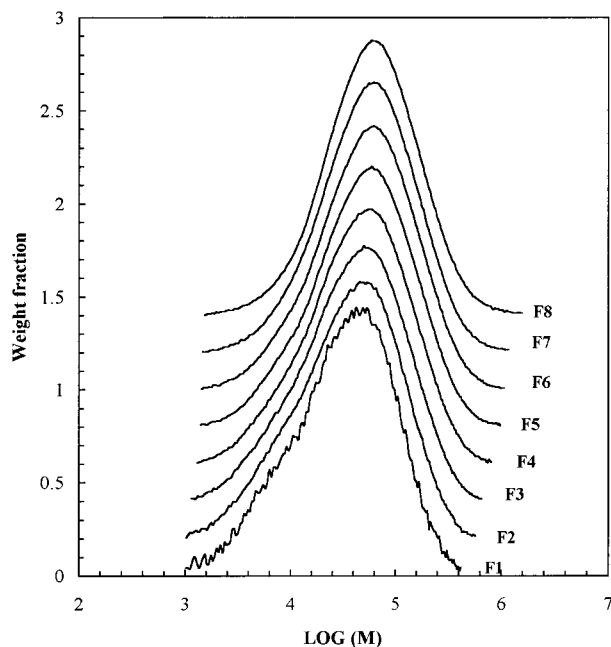


**Figure 4** Molar mass distribution of PTREF fractions of Ziegler-Natta LLDPE (PF0118F) obtained at various temperature intervals: F1, 30–50; F2, 50–60; F3, 60–70; F4, 70–75; F5, 75–80; F6, 80–85; F7, 85–90; and F8, 90–100°C.

above 30°C were very similar in shape. The curve for elution temperature of 20–30°C appeared at lower molar mass. Notice from Table IV that the fraction eluted between 40 and 45°C had the highest molar mass. The polydispersity for all the fractions was very similar in magnitude. The TREF fractions of the metallocene sample had narrower molar mass distributions than those of the Ziegler-Natta sample, as indicated by polydispersity values.

**Table III** Molar Masses and Polydispersity of the PTREF Fractions of the Ziegler-Natta LLDPE

Fraction	$T_e$ (°C)	$M_n \cdot 10^{-4}$	$M_w \cdot 10^{-4}$	$P_d$
F1	30–50	1.63	5.86	3.59
F2	50–60	1.86	6.70	3.60
F3	60–70	2.03	7.31	3.60
F4	70–75	2.42	8.46	3.50
F5	75–80	2.80	9.52	3.40
F6	80–85	3.07	9.87	3.21
F7	85–90	3.43	10.39	3.03
F8	90–100	3.82	10.94	2.86

$T_e$ , elution temperature range of PTREF.

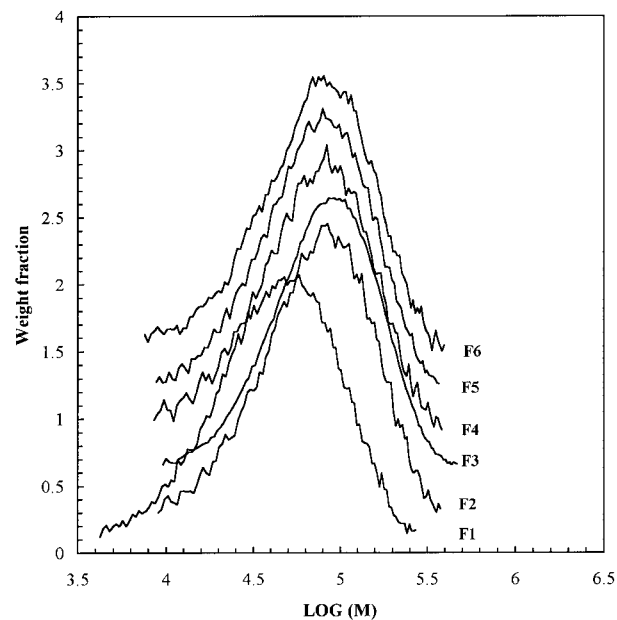


**Figure 5** Molar mass distribution of PTREF fractions of metallocene LLDPE (Exact4033) obtained at various temperature intervals: F1, 20–30; F2, 30–40; F3, 40–45; F4, 45–50; F5, 50–55; and F6, 55–60°C.

The relationship between molar mass and short chain branching distribution for the two different LLDPEs can be elucidated by plotting the weight average molar mass of PTREF fractions against the degree of SCB (Fig. 6). It can be seen that the  $M_w$  of the Ziegler-Natta sample increased monotonically with the decrease in the degree of short chain branching. This result is in agreement with results generally found on commercial Ziegler-Natta samples.<sup>5,6,9</sup> However, for the metallocene sample, there appeared to be a maximum in the plot of  $M_w$  vs SCB. Cross-fractionation of three other commercial metallocene LLDPEs resulted in the same trend (see Fig. 6), suggesting that the observed relationship of a

**Table IV** Molar Masses and Polydispersity of the PTREF Fractions of the Metallocene LLDPE

Fraction	$T_e$ (°C)	$M_n \cdot 10^{-4}$	$M_w \cdot 10^{-4}$	$P_d$
F1	20–30	4.10	7.34	1.81
F2	30–40	5.81	10.07	1.73
F3	40–45	7.69	12.41	1.61
F4	45–50	7.04	10.50	1.50
F5	50–55	7.02	10.74	1.53
F6	55–60	6.75	10.81	1.60

maximum in the  $M_w$  vs the SCB plot is characteristic of metallocene LLDPE.

### TREF-SNA-DSC Cross-Fractionation

The heterogeneity of the comonomer or SCB distribution is an important characteristic in describing the molecular structure of LLDPE. There are two types of heterogeneities existing on the chain of LLDPE: intra- and intermolecular heterogeneity. Intramolecular heterogeneity means that the SCB distribution of individual macromolecule in the system is not uniform along the chain backbone. Intermolecular heterogeneity means that the SCB distribution differs from one molecule to another. As indicated above, the SNA-DSC segregates LLDPE molecules according to methylene sequence length. Therefore, unlike TREF, which can only evaluate intermolecular heterogeneity, the SNA-DSC is able to assess both intra- and intermolecular heterogeneity.

Figure 7 shows the SNA-DSC endotherms of PTREF fractions of the Ziegler-Natta LLDPE. The TREF elution temperature range and the SNA-DSC results are summarized in Table V. Note that the crystallinity of TREF fractions increased with elution temperature, as expected. Given the fact that the TREF fractions were collected at relatively narrow temperature intervals, it is reasonable to assume that the macromolecules represented by each TREF fraction have similar SCB distributions, and thus similar average SCB contents. Thus, the DSC endotherm of each fraction will represent the methylene se-

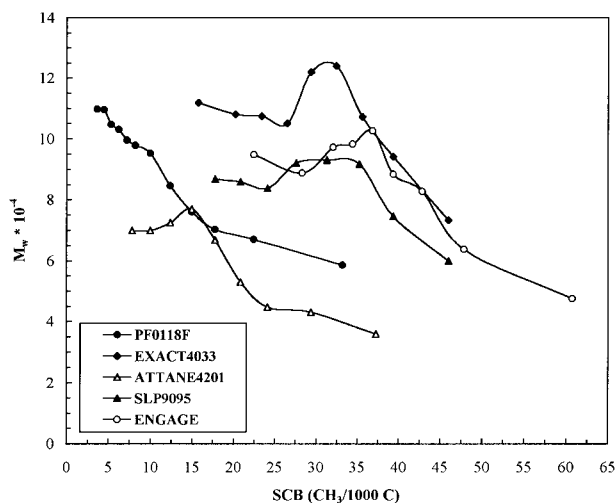


**Figure 6**  $M_w$  as a function of SCB for Ziegler-Natta and metallocene LLDPEs.

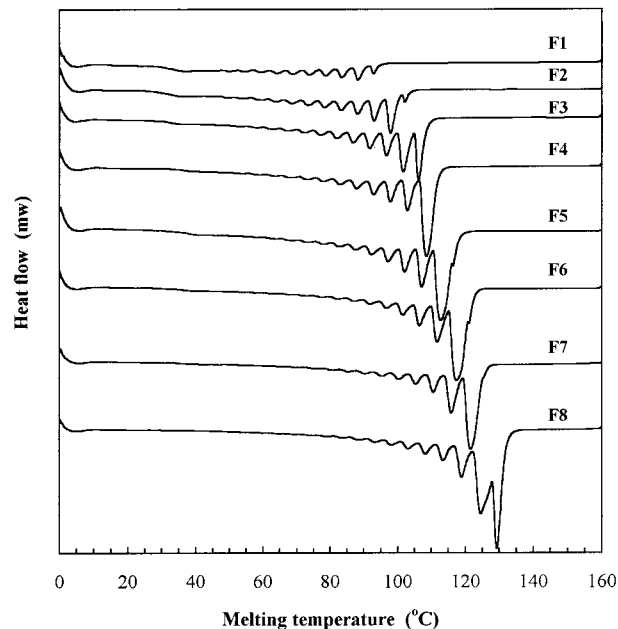


**Figure 7** DSC endotherms of PTREF fractions of Ziegler-Natta LLDPE obtained at various temperature intervals: F1, 30–50; F2, 50–60; F3, 60–70; F4, 70–75; F5, 75–80; F6, 80–85; F7, 85–90; and F8, 90–100°C.

quence distribution of all the molecules in the fraction regardless of molar mass. It is clear from Figure 7 that the molecules eluted at each temperature interval showed a distinctive methylene sequence distribution, indicating that the Ziegler-Natta LLDPE was intramolecularly heterogeneous. Also shown in Figure 7, the methylene sequence distribution varied considerably among fractions. The SNA-DSC endotherm of the fraction eluted between 30 and 50°C showed multiple peaks and a nearly symmetrical distribution of methylene sequence. With the increase in the elution temperature, the peaks of higher melting temperature became dominant in intensity. Moreover, the spectrum of the endotherms shifted toward high temperature. Clearly, the Ziegler-Natta LLDPE is intermolecularly heterogeneous in terms of methylene sequence distribution as well. The results suggest that the Ziegler-Natta LLDPE is a mixture of macromolecules of very different SCB distribution, and a single distribution function as reported in the literature<sup>21–23</sup> may not be sufficient to describe the heterogeneity.

The results also provide another possible interpretation of the TREF separation mechanism which has not yet been fully understood in the open literature.<sup>24–26</sup> Although it is generally

**Table V** TREF and SNA-DSC Results of the Ziegler-Natta Ethylene-Butene Copolymer

Fraction	$T_e$ (°C)	$T_{\text{onset}}$ (°C)	$T_{\text{peak}}$ (°C)	$\Delta H_u$ (J/g)	$X_c$ (%)
F1	30–50	86.6	88.3	58.0	20.2
F2	50–60	96.3	98.0	84.2	29.3
F3	60–70	104.2	105.7	106.5	37.1
F4	70–75	106.6	108.6	113.1	39.4
F5	75–80	110.6	112.8	119.7	41.7
F6	80–85	115.1	117.5	124.1	43.2
F7	85–90	119.5	121.6	138.4	48.2
F8	90–100	127.9	129.6	156.1	54.4

$T_{\text{onset}}$ , onset temperature of the primary peak on DSC endotherm;  $T_{\text{peak}}$ , peak temperature of the primary peak on DSC endotherm;  $\Delta H_u$ , heat of fusion;  $X_c$ , crystallinity.

agreed that TREF fractionates semicrystalline polymer based on crystallizability, and so most of the TREF calibrations have been based on the average SCB generated from PTREF,<sup>1,2</sup> there has been suggestions that TREF separates macromolecules based on the length of the crystallizable sequence.<sup>25,26</sup> This can be easily understood by considering a crystallized molecule in the TREF column; only when the longest sequence in the molecule dissolves does the whole molecule elute from the column. As shown in Figure 7, the shifting of the methylene sequences toward high elution temperatures or long sequences implies that the longest methylene sequence length may dictate the separation by TREF.

The SNA-DSC endotherms of PTREF fractions of the metallocene LLDPE are shown in Figure 8, and the TREF elution temperature and the SNA-DSC results are listed in Table VI. There was a narrow methylene sequence distribution within the molecules of each fraction. Also, it is very intriguing to see all TREF fractions appeared to show the same distribution. These results clearly suggest, in a rather direct manner, that the metallocene LLDPE has only intramolecular heterogeneity in chemical composition. In other words, the metallocene LLDPE is composed of macromolecules possessing the same SCB distribution, and therefore one can use one distribution function to describe the compositional heterogeneity. A similar conclusion has been deduced recently from TREF-<sup>13</sup>C nuclear magnetic resonance of metallocene LLDPE.<sup>7</sup>

The distinctive difference in methylene sequence distribution between the Ziegler-Natta and metallocene LLDPEs can be better understood by considering the very different nature of the two catalyst systems. As mentioned above, there are multiple active sites present on the

Ziegler-Natta catalyst,<sup>2,7,17</sup> whereas the metallocene catalyst is generally believed to have a single type of catalytic site. According to the instantaneous bivariate distribution theory for the composition of linear copolymer proposed by Stockmayer and used by others,<sup>21–23</sup> a single catalytic site produces copolymer with a narrow distribution in both molar mass and composition. Thus, it is understandable that the LLDPE produced by the single-sited metallocene catalyst shows only narrow molar mass distribution and intramolecular heterogeneity. For the Ziegler-Natta catalyst

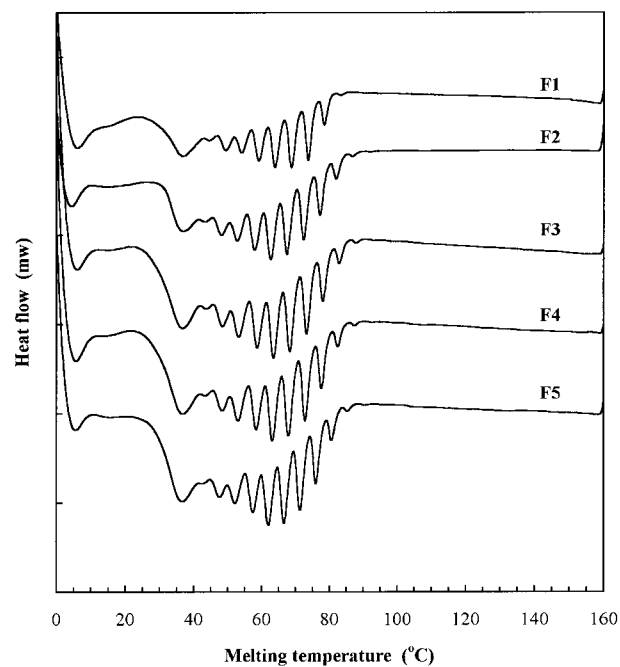


**Figure 8** DSC endotherms of PTREF fractions of metallocene LLDPE obtained at various temperature intervals: F1, 30–40; F2, 40–45; F3, 45–50; F4, 50–55; and F5, 55–65°C.

**Table VI TREF and SNA-DSC Results of Metallocene Ethylene-Butene Copolymer**

Fraction	$T_e$ (°C)	$T_{\text{onset}}$ (°C)	$T_{\text{peak}}$ (°C)	$\Delta H_u$ (J/g)	$X_c$ (%)
F1	30–40	—	—	—	—
F2	40–45	59.7	62.7	33.10	11.5
F3	45–50	60.3	63.5	37.79	13.2
F4	50–55	60.0	63.2	38.65	13.5
F5	55–65	58.6	62.0	40.54	14.1

having multiple sites, each site presumably produces molecules of intramolecular heterogeneity, whereas it is likely that different sites produce polymer with different SCB distributions. This seems to be evidenced by the very different methylene sequence distribution of the PTREF fractions of the Ziegler-Natta LLDPE as shown in Figure 7.

## CONCLUSIONS

TREF-SNA-DSC cross-fractionation is an effective way of fractionating semicrystalline polymer based on both crystallizability and chain sequence length. It can provide, in a rather direct manner, detailed information about the SCB distribution heterogeneity of different types of LLDPEs.

TREF-SNA-DSC cross-fractionation demonstrates that the metallocene LLDPE possessed only intramolecular heterogeneity, whereas the Ziegler-Natta LLDPE showed both intra- and intermolecular heterogeneity. TREF-SEC cross-fractionation showed that the molar mass of the Ziegler-Natta LLDPE decreases with increasing degree of branching, whereas the plot of molar mass vs SCB for metallocene LLDPE appears to show a characteristic maximum. The pronounced difference in molar mass and SCB distribution between the two LLDPEs well reflects the difference in catalytic properties of Ziegler-Natta and metallocene catalysts.

The authors thank Mrs. N. Bu for measuring the molar masses by SEC. The support of this work by the Natural Sciences and Engineering Research Council of Canada and NOVA Chemicals Corporation is gratefully acknowledged.

## REFERENCES

- Wild, L. *Adv Polym Sci* 1991, 98, 1–47.
- Soares, J. B. P.; Hamielec, A. E. *Polymer* 1995, 36, 1639–1654.
- Usami, T.; Gotoh, Y.; Takayama, S. *Macromolecules* 1986, 19, 2722–2726.
- Todo, A.; Kashiwa, N. *Macromol Symp* 1996, 101, 301–308.
- Karbaszewski, E.; Kale, L.; Rudin, A.; Tchir, E. J.; Cook, D. G.; Pronovost, J. O. *J Appl Polym Sci* 1992, 44, 425–434.
- Mirabella, F. M., Jr.; Ford, E. A. *J Polym Sci, Part B: Polym Phys* 1990, 25, 777–790.
- Balbontin, G.; Camurati, I.; Dall'Occo, T.; Ziegler, R. C. *J Mol Catal A: Chem* 1995, 98, 123–133.
- Kapoglanlan, S. A.; Harrison, I. R. *Polym Eng Sci* 1996, 36, 731–736.
- Mingozzi, I.; Nascetti, S. *Int J Polym Anal Charact* 1996, 3, 59–73.
- Huang, J. C. K.; Lacombe, Y.; Lynch, D. T.; Wanke, S. E. *Ind Eng Chem Res* 1997, 36, 1136–1143.
- Shaw, B. M.; McAuley, K. B.; Bacon, B. W. *Polym React Eng* 1998, 6, 113–142.
- Wild, L.; Ryle, T. R.; Knobeloch, D. C.; Peat, I. R. *J Polym Sci, Polym Phys Ed* 1982, 20, 441–455.
- Hosoda, S. *Polym J* 1988, 20, 383–397.
- Adisson, E.; Ribeiro, M.; Deffieux, A.; Fontanille, M. *Polymer* 1992, 33, 4337–4342.
- Keating, M. Y.; McCord, E. E. *Thermochim Acta* 1994, 243, 129–145.
- Keating, M. Y.; Lee, I-Hwa; Wong, C. S. *Thermochim Acta* 1996, 284, 47–56.
- Starch, P. *Polym Int* 1996, 40, 111–122.
- Muller, A. J.; Hernandez, Z. H.; Arnal, M. L.; Sanchez, J. J. *Polym Bull* 1997, 39, 465–472.
- Zhang, M.; Huang, J. C. K.; Lynch, D. T.; Wanke, S. E. *ANTEC '98, 1998, 2000–2003*.
- Fillon, B.; Wittmann, J. C.; Thierry, A. *J Polym Sci, Part B: Polym Phys* 1993, 31, 1383–1393.
- Stockmayer, W. H. *J Chem Phys* 1945, 13, 199–207.
- Soares, J. B. P.; Hamielec, A. E. *Macromol Theory Simul* 1995, 4, 305–324.
- Thomunn, Y.; Sernetz, F. G.; Thomunn, R.; Kressler, J.; Mulhaupt, R. *Macromol Chem Phys* 1997, 198, 739–748.
- Karbaszewski, E.; Rudin, A.; Kale, L.; Tchir, E. J. *Poly Eng Sci* 1993, 33, 1370–1371.
- Bonner, J. G.; Frye, C. J.; Capaccio, G. *Polymer* 1993, 34, 3532–3534.
- Elicabe, G.; Cordon, C.; Carella, J. *J Polym Sci, Part B: Polym Phys* 1996, 34, 1147–1154.